Bi-functional nonlinearities in monodisperse ZnO nano-grains – Self-consistent transport and random lasing

Andreas Lubatsch[1] and Regine Frank[2*] [1]

[1] *Georg-Simon-Ohm University of Applied Sciences, Keßlerplatz 12, 90489 Nürnberg, Germany,*
[2] *Institute for Theoretical Physics, Optics and Photonics, Eberhard-Karls-Universität, Auf der Morgenstelle 14, 72076 Tübingen, Germany*

Abstract.
We report a quantum field theoretical description of light transport and random lasing. The Bethe-Salpeter equation is solved including maximally crossed diagrams and non-elastic scattering. This is the first theoretical framework that combines so called off-shell scattering and lasing in random media. We present results for the self-consistent scattering mean free path that varies over the width of the sample. Further we discuss the density dependent correlation length of self-consistent transport in disordered media composed of semi-conductor Mie scatterers.

Keywords: disordered systems, transport theory, random lasing, non-equilibrium
PACS: 42.25.Dd, 42.55.Zz, 72.15.Rn, 78.20.Bh

INTRODUCTION

Random lasers and their coherence properties are recently investigated theoretically as well as experimentally [1, 2, 3, 4]. However efficient theoretical methods that may treat strongly scattering solid state random lasers, including non-linear gain and gain saturation, are still of urgent need. One ansatz to reach this goal is to employ methods from quantum field theory that have proven to be efficient in solving strong localization of photons in random [5, 6] and complex media [7, 8]. In this article we investigate the spatial coherence properties of different random laser samples theoretically. The samples only vary in their filling with spherical ZnO Mie scatterers. Besides the coherence within these systems we discuss the self-consistent scattering mean free path l_s of random lasers. We show that the scattering mean free path l_s of random lasers is not only a material characteristic and dependent to the filling as it has been often estimated in literature [9, 10, 11]. Instead it changes in depth of the sample and therefore depends on the nonlinear self-consistent gain in strongly scattering solid-state random lasers, especially at the surface.

MODEL

The theoretical model is based on an extended approach of the Bethe-Salpeter equation including maximally crossed diagrams. Additionally we model the scattering nano-grains by means of ZnO semi-conductor Mie spheres. This implies so-called off-shell scattering which is an implicit characteristic of a complex refractive indexed medium [12]. Consequently it leads to a renormalized condition for local energy conservation, the Ward identity for active Mie spheres [13]. We discuss how this approach can be expanded to a more sophisticated frame using non-equilibrium Keldysh theory in order to cover properly for locally occurring electromagnetically induced transparency (EIT).

The system we consider consists of a randomly scattering medium in the form of a slab geometry [14]. This slab is finite d sized in the z-dimension and assumed of to be of infinite extension in the (x,y) plane (see Fig.(1)). In experimentally relevant situations this refers to film structures of thickness up to 32 μm. The spherical Mie scatterers [15, 16] are embedded in a homogeneous host material which is considered to be passive. Both, scatterer and host medium, are described by means of a complex dielectric function ε_s and ε_b, respectively. The scatterers are modeled to

[1] Phone: +49-7071 / 29-73434; email: r.frank@uni-tuebingen.de; web: www.uni-tuebingen.de/photonics

15th International Conference on Transport in Interacting Disordered Systems (TIDS15)
AIP Conf. Proc. 1610, 147-152 (2014); doi: 10.1063/1.4893526

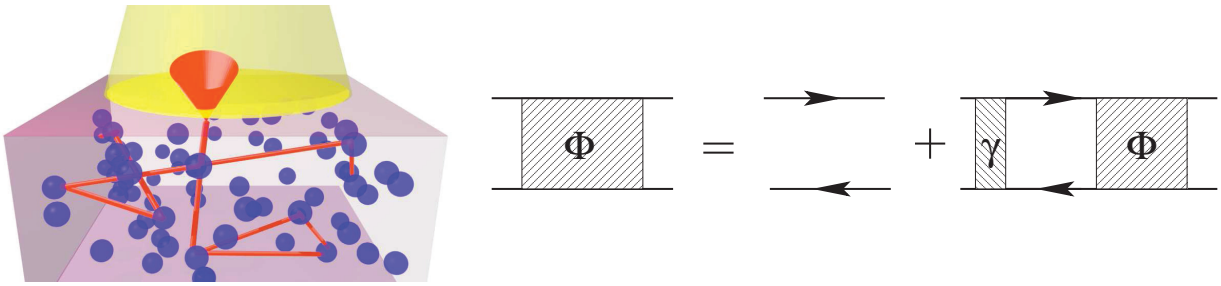

FIGURE 1. (a) ZnO spherical Mie scatterers at random locations (blue) are optically pumped from above (wide yellow beam). The pumping yields an inversion of the atomic occupation number within the ZnO causing stimulated emission of light (orange light paths). The emitted intensity multiply scatters and concentrates due to the samples density distributions. At the laser threshold the system experiences a phase transition and second order coherent intensity, meaning coherence in space and time, escapes the system through its surfaces (orange cone). The scatterers radius is $r_0 = 600nm$, $\lambda = 723nm$ and the samples finite dimension is of $d = 32\mu m$. (b) Diagrammatic representation of the Bethe-Salpeter equation. The four-point correlator Φ (on the left) is given as self-consistent integral over k and k' relating the Green's functions and the irreducible vertex γ including multiple scattering as well as all interference effects of time reversal processes (on the right).

be optically active ZnO, with a refractive index for the passive case of 2.1. The imaginary part of the permittivity $\mathrm{Im}\,\varepsilon_s$, comprised in the gain is self-consistently derived. This sample is optically pumped in order to achieve a sufficient electronic population inversion within the active medium of the scatterers by means of an incident pump laser, perpendicular onto the (x,y)-surface of the random laser. The laser feedback is guaranteed by multiple scattering. The same mechanism actually supports stimulated emission and hence coherent light intensity within the setup. The so generated laser intensity then may leave the sample through both open surfaces of the sample geometry, the dissipation channels. The emitted light is eventually observed at the surface of the sample in the form of lasing spots which comprise to a lasing mode. These lasing modes are of a characteristic size which is determined through this theory to be the correlation length ξ within the mass term of the diffusion pole. The latter depends only on system parameters such as scatterer size, wavelength of the pump source, filling fraction and film thickness.

The field-field correlation or coherence length of the propagating lasering intensity, is derived by means of the field theoretical approach of localization of photons based on the theory by Vollhardt and Wölfe [17]. Non-equilibrium band-structure calculations with a basic Hubbard model [18] for Zno bulk prove the existence density of states in the semi-conductor gap and optical gain for the non-equilibrium situation. The latter indicates electrical/optical induced transparency (EIT) processes for high energy pumping of solid state random lasers. Consequently no optical gap is observed. It is washed out due to uncorrelated disorder (see next section) and the mentioned non-equilibrium processes. In addition lasing especially in the semi-conductor gap may be observed, where non-equilibrium is not necessarily to be assumed in the laser model, however the stationary state defines the threshold of the laser.

TRANSPORT THEORY

The equation of motion for the electric field of stimulated emitted light $\Psi_\omega(\vec{r})$ within the sample is given by the wave equation

$$\frac{\omega^2}{c^2}\,\varepsilon(\vec{r})\Psi_\omega(\vec{r}) + \nabla^2\Psi_\omega(\vec{r}) = -i\omega\frac{4\pi}{c^2}\,j_\omega(\vec{r})\,, \tag{1}$$

where we denote c to be the vacuum speed of light and $j_\omega(\vec{r})$ the external source. The dielectric constant $\varepsilon(\vec{r}) = \varepsilon_b + \Delta\varepsilon\,V(\vec{r})$, where the dielectric contrast has been defined according to $\Delta\varepsilon = \varepsilon_s - \varepsilon_b$, including a random arrangement of scatterers in terms of $V(\vec{r}) = \sum_{\vec{R}} S_{\vec{R}}(\vec{r} - \vec{R})$, with $S_{\vec{R}}(\vec{r})$ a localized shape function at random locations $\vec{R}$. The intensity is then related to the field-field-correlation function Φ, often referred to as the four-point-correlation, $\Phi = \langle \Psi(\vec{r},t)\Psi^*(\vec{r}',t')\rangle$. Here, the angular brackets $\langle\ldots\rangle$ refer to the disorder average or ensemble average of this random system [19, 20]. In order to calculate the field-field-correlation Φ the Green's function formalism is best suited. The wavefunction of the electromagnetic field reads

$$\Psi(\vec{r},t) = \int \mathrm{d}^3r' \int \mathrm{d}t'\, G(\vec{r},\vec{r}';t,t')\,j(\vec{r}',t')\,. \tag{2}$$

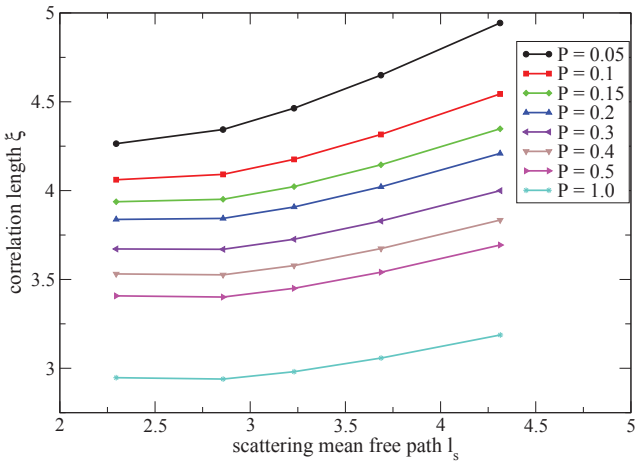

FIGURE 2. Calculated correlation length ξ of the random lasing modes as a function of the calculated scattering mean free path l_s. Both length scales are given in units of the scatterer radius r_0. Different curves correspond to different strengths of the pump intensity P, given in units of transition rate γ_{21}. The different points along a given curve correspond to different filling fractions of the zinc oxide scatterers. The symbols from left to right correspond to filling fractions of 60%, 50%, 45%, 40%, and 35%.

The single-particle Green's function Eq. (3) is related to the (scalar) electrical field, by inverting the (non-linear) wave equation Eq. (1) . It reads in in the density approximation of independent scatterers [5, 7]

$$G(\omega,\vec{q}) = \frac{1}{\varepsilon_b(\omega/c)^2 - |\vec{q}|^2 - \Sigma_{\vec{q}}^{\omega}} \tag{3}$$

where ω is the light frequency and ε_b is the dielectric function of the space in between the scatterers, $\vec{q}$ is the wave vector. $\Sigma_{\vec{q}}^{\omega} = n \cdot T$. T is the complex valued T-Matrix of the single scatterer, n is the volume filling fraction and $\Sigma_{\vec{q}}^{\omega}$ is the single particle self-energy including Mie scattering of the spheres coupled the non-linear response of the amplifying material. The scatterers are bi-functional in the sense that the semi-conductor structure amplifys light by generating light matter bound states yielding gain which renormalizes the resonance and leads to gain saturation. This behavior is typical for strongly scattering solid state random lasers comprised of pure semi-conductor powder and in theory it goes far beyond previously existing approaches, e.g. [1, 2].

In order to study transport in the above introduced field-field-correlation we consider the 4-point correlation function, defined now in terms of the non-averaged Green's functions, i.e. the retarded G^R and the advanced Green's function G^A, where now we find $\Phi \sim \langle G^R G^A \rangle$. The intensity correlation obeys an equation of motion itself, the Bethe-Salpeter equation (BS) [7], given in coordinate space given as

$$\Phi(r_1,r_1';r_2,r_2') = G^R(r_1,r_1')G^A(r_2,r_2') + \sum_{r_3,r_4,r_5,r_6} G^R(r_1,r_5)G^A(r_2,r_6)\gamma(r_5,r_3;r_6,r_4)\Phi(r_3,r_1';r_4,r_2'). \tag{4}$$

In the BS, we introduced the irreducible vertex function $\gamma(r_5,r_3;r_6,r_4)$ which represents all scattering interactions inside the disordered medium of finite size. The irreducible vertex is discussed in the given references in detail but we mention here that beyond ladder diagrams (*Diffuson*) so called maximally crossed diagrams (*Cooperons*) are included. This is actually a matter of course within the self-consistent theory of localization but it exceeds the usual description of the Bethe-Salpeter equation. Local controlled energy non-conservation is incorporated by means of the Ward identity [13]. To account for the particular form of the system geometry, Wigner coordinates are chosen, where a full Fourier transform of the spatial coordinates within the infinite extension of the (x,y)-plane is used. We use relative $\vec{q}_{||} = (q_x,q_y)$ and center-of-mass momentum $\vec{Q}_{||} = (Q_x,Q_y)$ variables. However, the finite z-coordinate of the slab is transformed into relative and center-of-mass real-space coordinates, i.e. z and Z respectively. In this representation only the relative coordinate is Fourier transformed. This procedure is justified because the relative coordinates of the intensity correlation are related to the scale of the oscillating electric field, whereas the center-of-mass coordinates are related to the scale of the collective behavior of intensity, which is a significantly larger scale. Given that the thickness

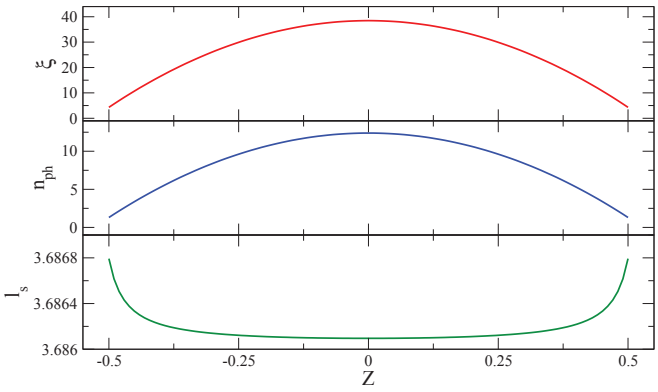

FIGURE 3. Calculated correlation length ξ, photon number density n_{ph} and scattering mean free path l_s across the slab geometry from surface to surface. The parameter set is a filling fraction of 40% and a pump rate of $P = 0.1\gamma_{21}$.

of the slab is much larger than the wavelength of the laser light as discussed above, a Fourier transform with respect to this perpendicular relative coordinate is perfectly acceptable. In this representation the BS equation, Eq. (4), may be rewritten according to

$$\left[\Delta\Sigma + 2\mathrm{Re}\,\varepsilon\omega\Omega - \Delta\varepsilon\omega^2 - 2\vec{p}_{||}\cdot\vec{Q}_{||} + 2ip_z\partial_Z\right]\Phi^{Q_{||}}_{pp'}(Z,Z') \tag{5}$$
$$= \Delta G_p(Q_{||};Z,Z')\delta(p-p') + \sum_{Z_{34}}\Delta G_p(Q_{||})\int\frac{\mathrm{d}p''}{(2\pi)^3}\gamma^{Q_{||}}_{pp''}(Z,Z_{34})\Phi^{Q_{||}}_{p''p'}(Z_{34},Z')$$

where we used the abbreviation $\Delta G \equiv G^R - G^A$. The rewritten BS equation, Eq. (6), also known as kinetic equation, therefore is seen to be a differential equation in finite center-of-mass coordinate Z along the limited dimension of the slab. This differential equation is accompanied by suitable boundary conditions accounting for the reflectivity of the sample surfaces. Eq. (6) is solved in terms of an expansion of the correlation Φ into its moments, identified as energy density and energy current density correlation, respectively. A self-consistent expression for the diffusion constant is derived, accompanied by a pole structure within the energy density expression.

$$\Phi_{\varepsilon\varepsilon}(Q,\Omega) = \frac{N_\omega(Y)}{\Omega + iDQ^2 - iD\xi^{-2}}. \tag{6}$$

The last term in the denominator $-iD\xi^{-2}$ is the so called mass term which is present for all kinds of complex media and off-shell scattering.

T-MATRIX AND LASING

The scattering properties of the disordered sample are included by means of an independent scatterer approximation. $\Sigma = n \cdot T$, where T is the complex valued T-Matrix of the single Mie sphere [13], necessarily this is "off-shell". The conservation laws are represented by the Ward identity. The incorporation of the lasing properties go by far beyond that approach. Even though the equations look uncomplicated, the numerical efforts for convergency of the 3-dimensional system are non-trivial. The lasing behavior in terms of the atomic occupation number is described by means of the following four-level laser rate equations [21]

$$\frac{\partial N_3}{\partial t} = \frac{N_0}{\tau_P} - \frac{N_3}{\tau_{32}} \tag{7}$$
$$\frac{\partial N_2}{\partial t} = \frac{N_3}{\tau_{32}} - \left(\frac{1}{\tau_{21}} + \frac{1}{\tau_{nr}}\right)N_2 - \frac{(N_2 - N_1)}{\tau_{21}}n_{ph} \tag{8}$$

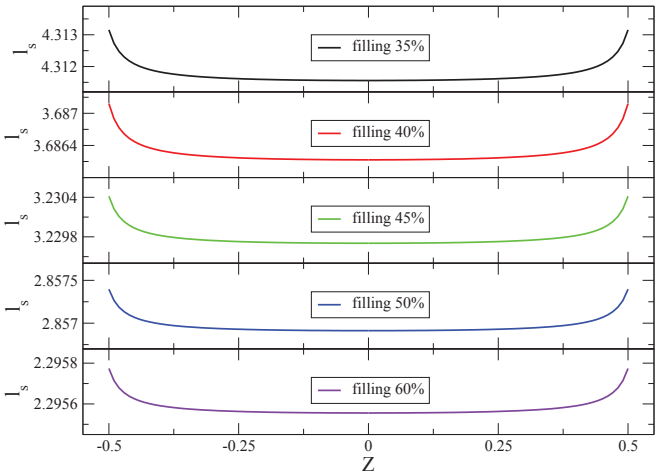

FIGURE 4. Calculated scattering mean free path l_s across the depth Z of the random lasing film for various filling fractions as indicated in the legends. The pump rate is set to be $P = 0.5\gamma_{21}$. l_s dependends on the atomic inversion, i.e. on the depth dependent imaginary part of the dielectric function $\mathrm{Im}\,\varepsilon_s$, which has been self-consistently calculated.

$$\frac{\partial N_1}{\partial t} = \left(\frac{1}{\tau_{21}} + \frac{1}{\tau_{nr}}\right) N_2 + \frac{(N_2 - N_1)}{\tau_{21}} n_{ph} - \frac{N_1}{\tau_{10}} \tag{9}$$

$$\frac{\partial N_0}{\partial t} = \frac{N_1}{\tau_{10}} - \frac{N_0}{\tau_P} \tag{10}$$

where $N_{tot} = N_0 + N_1 + N_2 + N_3$, $N_i = N_i(\vec{r},t)$, $i = 0,\ 1,\ 2,\ 3$ are the population number densities of the corresponding electron level; N_{tot} is the total number of electrons participating in the lasing process, $\gamma_{ij} \equiv 1/\tau_{ij}$ are the transition rates from level i to j, and γ_{nr} is the non-radiative decay rate of the laser level 2. $\gamma_P \equiv 1/\tau_P$ is the transition rate due to homogeneous, constant, external pumping. Further $n_{ph} \equiv N_{ph}/N_{tot}$ is the photon number density, normalized to N_{tot}. The four level system is chosen, because the stationary state, the threshold is easily established, i.e. $\partial_t N_i = 0$, hence the above system of equations can be solved for the population inversion $n_2 = N_2/N_{tot}$ to yield $n_2 = \frac{\gamma_P}{\gamma_P + \gamma_{nr} + \gamma_{21}(n_{ph}+1)}$, where it was assumed that γ_{32} and γ_{10} are large compared to any other decay rate.
In the last step the laser rate equations are coupled to the microscopic transport theory by identifying the growth term in the photon diffusion with corresponding growth term in the derived equation for the energy density correlation $\gamma_{21} n_2 = D/-\xi^2$. The equality is ensured by finding an approbate self-consistent imaginary part of the scatterers dielectric function $\mathrm{Im}\,\varepsilon_s$ for any particular light frequency ω and any position Z within the slab geometry.

The here developed theory of random lasing includes the regular self-consistency of the Vollhard-Wölfe type for the diffusion coefficient including the interference effects of emitted light intensity. The self-consistent results for the imaginary part $\mathrm{Im}\,\varepsilon_s$ of the dielectric coefficient of the laser active scatterers are derived by coupling the mesoscopic transport to semiclassical laser rate equations. The single particle self-energy $\Sigma(\omega)$ entering the single particle Green's function, as in Eq. (3), is approximated as $\Sigma = n \cdot T$, where n is the volume filling fraction of scatterers in the host medium and T is the T-matrix of the Mie scatterer. These internal resonances are renormalized, but nevertheless they allow for low and stable laser thresholds. In Fig. 2 the calculated correlation length ξ is given in units of the scatterer radius r_0 and presented as a function of the scattering mean free path l_s of the random system. The bullets on the curves correspond to several filling fractions. We find, that the correlation length increases with the mean free paths and again decreases with higher pump intensities. That behavior can be interpreted as self-balancing of sample energy at the threshold. On the abscissa l_s is given in units of the scatterer radius r_0.The different curves correspond to different strengths of the pump intensity P, given in units of transition rate γ_{21}. The displayed symbols along one graph correspond to numerical evaluations for different filling fractions of the zinc oxide scatterers. In particular, the points from left to right correspond to filling fractions of 60%, 50%, 45%, 40%, and 35%. The correlation or coherence length is found to decrease with increasing pump intensity. Further, the dependence on the scattering mean free path is decreased for stronger pumping. This is in agreement with recent experimental results, as discussed in reference [3]. The correlation length ξ at the surface of the sample, Fig. 2, is displayed in Fig. 3 across the sample thickness for a

volume filling fraction of the scatterer of 40% and a pump rate of $P = 0.1\gamma_1$ in the upper panel. This is accompanied by the calculated photon number density in the middle panel as well as the scattering mean free path l_s as a function of the sample depth Z. The self-consistent scattering mean-free path l_s Fig. 4 is displayed for various filling fractions 35%..60%. The density dependency can be clearly observed, but additionally and even more important the variation of the scattering mean free path l_s across the width of the sample is especially noteworthy. It clearly shows the influence of lossy boundaries on the inversion and therefore the self-consistent gain and gain saturation depending on the position. Near the surface the mean free path is in units of r_0 increasing. However it increases counter-intuitively stronger for low filling fractions. Consequently the approach of some ballistic limes in low filling raises expectations that the lossy boundary will gain importance. This is an important result which has not been reported before.

CONCLUSION

In summary, we considered a system of randomly positioned laser active ZnO scatterers and we developed a systematic theory for random lasing in finite sized disordered systems. The self-consistent theory of light localization, including interference effects, is coupled to the laser rate equation in order to obtain the corresponding nonlinear gain of the lasing system. The calculated averaged correlation length of the occurring lasing spots is systematically studied and found to exhibit a characteristic dependence on the scattering mean free path of the sample in dependency to the in-depth position. Further the self-consistent scattering mean free path l_s depends on the position with respect to lossy boundaries. Therefore we conclude that the complex valued T-matrix "off-shell" of the single scatterer in self-consistent stationary state significantly varies across the sample and therefore the scattering strength of the particle is driven by so-called electromagnetically induced transparency processes (EIT) which obviously occur not only in high non-equilibrium of the ultrafast regime, but they do also occur due the amount of coherent intensity present in the scattering sample. The latter is for homogeneous pumping higher in the samples center.

REFERENCES

1. H. E. Türeci *et al.*, "Strong Interactions in Multimode Random Lasers", *Science* **320**, 643 (2008).
2. P. Stano, P. Jacquod, "Suppression of interactions in multimode random lasers in the Anderson localized regime", *Nature Photonics*, **7**, 66-71 (2013).
3. B. Redding, M. A. Choma, H. Cao, "Spatial coherence of random laser emission", *Optics Letters* **36**, 3404 (2011).
4. S. Aberra Guebrou *et al.*, "Coherent Emission from a Disordered Organic Semiconductor Induced by Strong Coupling with Surface Plasmons", *Phys. Rev. Lett.* **108**, 066401 (2012).
5. B. A. van Tiggelen *et al.*, "Effect of Resonant Scattering on Localization of Waves", *Europhys. Lett.* **15** (5), 535-540 (1991).
6. M. P. van Albada *et al.*,"Speed of Propagation of Classical Waves in Strongly Scattering Media", *Phys. Rev. Lett.* **66**, 24, 3132 (1991).
7. R. Frank, A. Lubatsch, "Scalar Wave Propagation in Random, Amplifying Media: Influence of Localization Effects on Length and Time Scales and Threshold Behavior", *Phys. Rev. A* , **84**, 013814 (2011).
8. G. Maret, *et al.*, "Reply: Inelastic scattering puts in question recent claims of Anderson localization of light ",*Nature Photonics* **7**, 934 (2013).
9. S. Fiebig *et al.*, "Conservation of energy in coherent backscattering of light" *EPL* **81**, 64004 (2008).
10. X. H. Wu *et al.*,*Random lasing in closely packed resonant scatterers*, J. Opt. Soc. Am. B **21**, 159 (2004).
11. J. Fallert *et al.*, "Co-existence of strongly and weakly localized random laser modes" *Nature Photonics* **3**, 279 (2009).
12. J. J. Sakurai, J. Napoletano, "Modern Quantum Mechanics" *Pearson* **3**, 279 (2011).
13. A. Lubatsch, H. Kroha, K. Busch,"Theory of light diffusion in disordered media with linear absorption or gain" *Phys. Rev. B* **71**, 184201 (2005).
14. D. S. Wiersma, "The physics and applications of random lasers" *Nature Physics* **4**, 359 (2008).
15. G. Mie, "Beiträge zur Optik trüber Medien, speziell kolloidaler Metallösungen" *Annalen der Physik* , **4** , 25, 377-445 (1908).
16. K. L. van der Molen *et al.*, "Laser threshold of Mie resonances." *Opt. Lett.* **31**, 1432 (2006).
17. D. Vollhardt and P. Wölfle, "Diagrammatic, self-consistent treatment of the Anderson localization problem in $d <= 2$ dimensions.", *Phys. Rev. B* **22**, 4666 (1980).
18. R. Frank, "Coherent control of Floquet-mode dressed plasmon polaritons" *Physical Review B* **85**, 19, 195463 (2012).
19. P. Sheng, "Introduction to wave scattering, localization and mesoscopic phenomena", *Springer* (2006).
20. J. B. Jalickee, T. Morita, T. Tanaka, "On the configurational average of the Green's function for liquid metals", *Philosophical Magazine*, **12:115**, 209-212 (1965).
21. A. E. Siegman, "Lasers", *Stanford University Press* (1986).